ACCEPTED BY ASTROPHYSICAL JOURNAL LETTERS.
Preprint typeset using LaTeX style emulateapj v. 10/09/06

STOCHASTICALLY INDUCED GAMMA-RAY BURST WAKEFIELD PROCESSES

JACOB TRIER FREDERIKSEN
Stockholm Observatory, AlbaNova University Center, SE-106 91 Stockholm, Sweden
Accepted by Astrophysical Journal Letters.

ABSTRACT

We present a numerical study of Gamma-Ray Burst - Circumburst Medium interaction and plasma preconditioning via Compton scattering. The simulation tool employed here – the PHOTONPLASMA code – is a unique hybrid model; it combines a highly parallelized (Vlasov) particle-in-cell approach with continuous weighting of particles and a sub-Debye Monte-Carlo binary particle interaction framework. Our first results from 3D simulations with this new simulation tool suggest that magnetic fields and plasma density filaments are created in the wakefield of prompt gamma-ray bursts, and that the photon flux density gradient has a significant impact on particle acceleration in the burst head and wakefield. We discuss some possible implications of the circumburst medium preconditioning for the trailing afterglow, and also discuss which additional processes will be needed to improve future studies within this unique and powerful simulation framework.

Subject headings: Gamma rays: bursts – plasmas – magnetic fields – methods: numerical – instabilities – acceleration of particles

1. INTRODUCTION

The microphysics of Gamma-Ray Burst (GRB) afterglow shocks propagating through a circumburst medium (CBM) has been theoretically predicted by (Medvedev & Loeb 1999) and later extensively studied using particle-in-cell (PIC) models in the past few years (see e.g. Keshet et al. 2008; Hededal et al. 2004; Frederiksen et al. 2004; Silva et al. 2003; Gruzinov 2001). In contrast, the initial interaction between the GRB photons and the CBM plasma is less well studied numerically, although progress has been made for coherent wakefield processes in lower-dimensional and pair plasmas (e.g. Hoshino 2008; Liang & Noguchi 2007). Whereas the burst-CBM interaction has received strong attention in theoretical (Beloborodov 2002; Thompson & Madau 2000) and observational (Connaughton 2002) works, the detailed microphysical plasma dynamics in the first pulse-plasma encounter lacks sufficient treatment with respect to the high degree of forcing anisotropy in the problem of photon scattering off the relatively cold tenuous CBM.

Wakefield interactions between high energy photon pulses and a plasma have been extensively studied in the context of *coherent* wakefield acceleration in laser-plasma systems, both experimentally (e.g. Phuoc et al. 2005; Kostyukov et al. 2003), and numerically in the same context (e.g. Phuoc et al. 2005; Pukhov 2000). In the astrophysical context of particle acceleration in GRBs, wakefield acceleration has been studied in the coherent regime where the forcing of the plasma is done by the electromagnetic field (Hoshino 2008; Liang & Noguchi 2007). Incoherent – or *stochastic* – wakefield processes have to our knowledge so far not been studied numerically, and has been considered theoretically only in a few cases (e.g. Barbiellini et al. 2006, 2004).

Our motivation for developing a new and improved Particle-in-cell- Monte-Carlo (PIC-MC) code framework for investigating the detailed Compton interaction of an ultra-intense GRB and a quiescent cold CBM is two-fold:

First, due to the high-energy spectrum of the prompt GRB (for BATSE of order $E_\gamma \sim m_e c^2$), the photon wavelength is much shorter than any characteristic length scale in the CBM plasma, $\lambda_\gamma \ll \delta_e$ and $\lambda_\gamma \ll \lambda_D$, where δ_e and λ_D are the electron skin-depth and Debye-length, respectively. We therefore expect a binary approximation to work well for prompt burst photons interacting with the plasma constituent particles through Compton scattering. In fact, photons in a large range down towards the electron plasma frequency $\omega_\gamma \sim \omega_{pe} = \lambda_D^{-1} v_{th,e}$ (where $v_{th,e}$ is the electron thermal speed) could be treated as point particles that interact in a binary way with the plasma.

Secondly, the extreme intensity of the burst makes the GRB front opaque to the plasma electrons. Assume a CBM with $n_e \approx 1$ cm^{-3}, and further assume a typical BATSE GRB with an estimated (from Barbiellini et al. 2006, eqn.2) photon flux energy density of 10^{35} eV cm^{-2} s^{-1} at distance $R_0 \sim 10^{16}$ cm from the progenitor. Then, Compton scattering off the CBM plasma will occur many times every second per electron during the prompt phase; most photons survive traversing the plasma without being significantly affected. The plasma is forced predominantly by binary particle- particle encounters, everywhere locally.

These considerations motivated us to develop and employ a new and unique tool in order to gain access to the sub-Debye regime. Adopting the "random phase approximation" (Pines & Bohm 1952) we may split, in a natural way, plasma processes into two different numerical schemes depending on the characteristic scale of the dynamics, here denoted $\mathbf{k}_C$:

- $\lambda_D \ll |\mathbf{k}_C|^{-1}$**:** for forcing and disturbances scale larger than the Debye length the Vlasov approach is applied and the PIC code framework is utilized.
- $\lambda_D \gg |\mathbf{k}_C|^{-1}$**:** in the opposite case dynamics is particle-particle interaction dominated, and we solve the scattering problem statistically through MC radiative transfer for the plasma constituents.

In this way we obtain a substantially improved description of the plasma for both the Vlasov and detailed balance cases, and capture in a natural way the details of wave-particle interaction and scattering. The PHOTONPLASMA code is parallelized with MPI and is highly scalable. Any plasma

Electronic address: jacob@astro.su.se / trier@astro.ku.dk

constituent species, forcing and scattering process is possible to incorporate with relative ease; for further details see (Haugboelle 2005; Frederiksen 2008).

In the remainder of this Letter we present, in Section 2, some central details on our numerical approach, and account for the simulation setup as well as physical and numerical scaling. Results and discussion are given in Section 3, where we also relate the wakefield effects to other results concerning coherent – rather than stochastically induced – wakefield processes. Conclusions are given in Section 4.

2. THE STOCHASTIC WAKEFIELD SIMULATION

Here we describe the 3D runs from our first wakefield experiments, full details of this as well as other setups, tests and more results can be found in Frederiksen (2008).

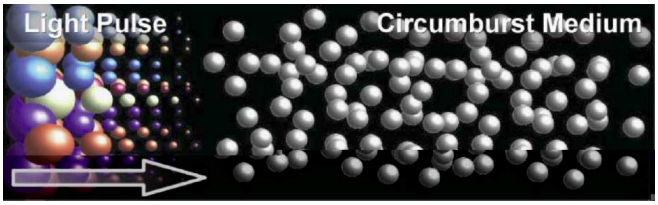

FIG. 1.— Illustration of our computational setup; GRB photons (left) move through the ambient CBM plasma. As the intensity of the light pulse increases, the *weights* (size) of the photons vary, rather than the *number*. Color designates that photons carry different energies (through ν) as well.

A synthetic thermal GRB is delivered to a quiescent CBM plasma by adding photons (particles) to the computational domain on a volume boundary, as illustrated in figure Fig. 1, according to a prescribed light curve and spectrum.

The light curve is inspired by BATSE data fitted to a FRED function (Kocevski et al. 2003; Ryde & Svensson 2002) with parameters chosen for BATSE trigger 3891, $r = 1.26$ and $d = 2.67$. The spectral window coincides with the BATSE window, $E_\gamma \in [33.6\text{keV}, 3.36\text{MeV}]$ – after correction for an estimated redshift of $z \sim 1.68$. The spectrum is assumed to be Planckian: $N_\gamma(\nu,t) = (h\nu)^{-1}F(\nu,t) = (h\nu)^{-1}B_\nu(T(t),t)$, for the photon spectral radiance. We use the Stefan-Boltzmann law to model the temperature, $T(t) \propto F(t)^{1/4}$. Our model FRED has duration $\tau_{GRB} = 200$, corresponding to about 1% of T_{50} for trigger 3891.

We evolve our synthetic GRB by adding a *constant* number of photons per cell carrying *continuous* weights prescribed by the burst functions. Photon energies are sampled from MC integration of the (time-dependent) Planckian. The photon spectral radiance is then

$$n_\gamma(\nu,t) \propto \frac{F(\nu,t)}{\nu} \propto \sum_{i=1}^{N_\gamma(\nu,t)} w_i(\nu,t) \;\Rightarrow\; n_\gamma(\nu,t) \propto \sum_{i=1}^{N_\gamma(\nu)} w_i(t)\,,$$

using our assumptions about the thermal GRB. The last sum, split into assigning time-variable weights and frequency variability to individual particles, gives a high degree of flexibility compared to conventional PIC codes.

The CBM plasma is assumed to be a uniform density medium, consisting of a hydrogenic, fully ionized, moderate temperature plasma with $v_{th,e} \approx 0.1c$. We have adopted conventional PIC scaling, setting all relevant natural constants equal to unity, except the ion-to-electron mass ratio, which is $m_i/m_e = 256$. The initial number of particles is 40/cell/species, and the grid resolution $100\times20\times4000$; this translates to $\{L_x, L_y, L_z\} \approx \{12\delta_e \times 2\delta_e \times 500\delta_e\}$ for our choices of length units and plasma density. The burst duration in light travel length is $L_{GRB} \approx 64\delta_e$. A relatively flat volume aspect ratio is a compromise to ensure skin-depth resolution at the lowest possible grid size to give any 3D structure a chance of growing marginally without spending excess computing time. Boundary conditions are for the lower (upper) boundaries: plasma particles are specularly reflected (thermalized) and outgoing photons are removed. Fields are damped in a layer $\Delta L_z \sim 0.1\% L_z$ on the boundaries to avoid spurious wave interference.

Compton scattering is conducted through MC binary interaction, using the full Klein-Nishina expression. Photons and electrons are selected pairwise at random for scattering according to their weights. To achieve detailed balance, scattering is done by splitting the particles into a new part carrying the Compton scattered fraction of the old part (Haugboelle 2005), and an unscattered remaining part. We may write

$$w_{(\gamma,e),scatt} = w_{(\gamma,e),old} - w_{(\gamma,e),new}\,,$$

where the weights of scattered electrons and photons are equal pairwise. The particle scatter fraction per time step then satisfies

$$w_{(e,\gamma),scatt} \propto w_e w_\gamma \overline{\overline{\sigma_C}}(\mathbf{p}_e, \mathbf{p}_\gamma) c\Delta t\,,$$

where $\overline{\overline{\sigma_C}}(\mathbf{p}_e, \mathbf{p}_\gamma)$ denotes the microphysical Compton scattering matrix for photons and electrons in a given cell. For a scattering fraction of 10^{-6}, 10^{24} *physical* particles are scattered away from a 'mother' particle of size 10^{30}, for example; this illustrates the flexible and inherent continuous nature of the PHOTONPLASMA code.

3. RESULTS AND DISCUSSION

3.1. *Wakefield-Plasma Gradient Effects and Transients*

As the pulse interacts with the quiescent plasma, electrons are strongly forward Compton scattered. The plasma reacts electrostatically to restore the displacement by pulling the bulk of the electrons backwards anti-parallel to the burst propagation direction, while this is turn back-reacts on the photons. The effects can be seen as the 'dip' from $z = 1500$, and to the left, in figures 2 and 3, where scatter plots in momentum sub-space $\{z, |\mathbf{p}_z|\}$ are shown for electrons and photons, respectively. The scatter plots are from runs with twice the resolution and half the density of those for the main simulation (Section 2 and fig.4). The well resolved and longer skin-depth reveals strong electrostatic beating in the plasma parallel momentum. These beats last of order $\tau_b \sim \delta_e/c \sim 10^{-4}$s in the CBM rest frame, and particles caught in the wake reach Lorentz factors upward of $\gamma_e \sim 30$.

Forwardly accelerated plasma – above the yellow line in Fig. 2 – relaxes to $|p_{z,e}| \sim \pm m_e c$ in a pace proportional to the burst duration, in order to counter-act the bulk backwards flow (the 'dip') initiated by the photons. The plasma undergoes violent accelerations, to maintain charge-neutrality. Burst photons keep the electron population 'inflated' as long as photon free energy and anisotropy is available in the plasma; far downstream the 'inflated' non-thermal population lasts through the duration of our simulations.

The violent electrostatic acceleration of plasma electrons, due to the sharp gradient in photon pressure, will produce bremsstrahlung and synchrotron photons. In subsequent upscattering these photons will eventually also affect the spectrum (Barbiellini et al. 2006). More importantly, millisecond variability could – in our assumed environment – arise directly from the enhanced density variations, scattering and

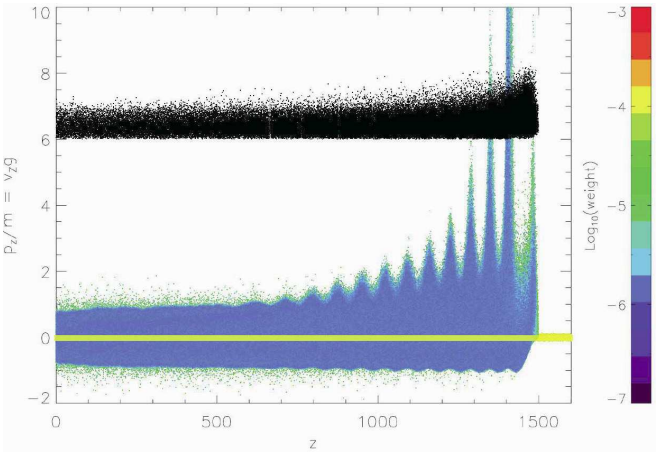

FIG. 2.— *Electron Scatter Plot*: Color designates weight in log-scale – blue particles have weights $w_{blue} \sim 10^{-5} w_0$, where w_0 is the initial weight. The yellow line coincides with zero bulk z-momentum, $p_{z,\gamma} = 0$. For clarity photons (black) are offset vertically by $p_{z,\gamma} = +6$.

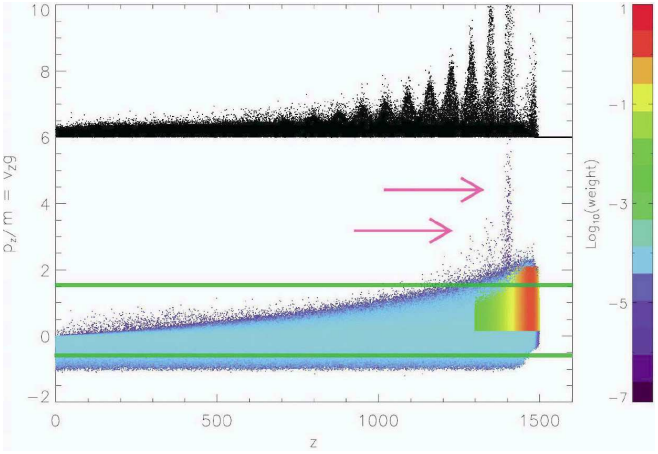

FIG. 3.— *Photon Scatter Plot*: same run as Fig. 2, but for photons (in color). The initial burst (moving right) is visible from $t \sim 1500$ to $t \sim 1300$. Pink arrows: local photon upscattering. Green lines: energy threshold for $\gamma+\gamma \rightarrow e^+ + e^-$ for photons pairwise oppositely outside (away from $p_z = 0$) these lines. Electrons (black) are offset by $p_{z,e} = +6$. Here, $p_{z,\gamma} \equiv [h\nu]_z/m_e c^2$.

possibly pair production (leading to higher densities and more scattering). Such a variability, which is comparable to the plasma frequency in a medium with density $n_0 \sim 10^{-1}\mathrm{cm}^{-3} - 10^{0}\mathrm{cm}^{-3}$, could therefore be self-feeding and grow in strength and duration. We may be observing a weak seed to such spike in the spectrum at high energy, marked by the two pink arrows in Fig. 3. Such photons spikes could facilitate pair production, and modify the GRB spectrum as the burst traverses the CBM.

3.2. *Magnetic Field Generation*

Most intriguingly, we observe growth of a strong, large-scale magnetic field in the downstream wakefield gradient region. The scenario is captured in Fig. 4. A cross section of the 3D volume is shown for electrons, photons, ions and the transverse magnetic field, $B_\perp$ (top-to-bottom), for the 3D run described in Section 2. Barely visible in the electron population is the same electrostatic spiky structure that shows in Fig. 2, but somewhat weaker due comparatively higher density and lower resolution.

From the ion density and electron density panels it is seen that both species undergo instability to form confluent filaments in the plasma (although the inertia difference plays a role). The filamentation build-up is initiated by fluctuating EM fields in CBM plasma ahead of the burst. As described in Section 3.1, the plasma forms a two-stream anisotropy in reaction to the burst forcing. The fastest growing instability in this case is the two-stream filamentation mode – tantamount to the Weibel instability (Weibel 1959) – which produces quasi-static magnetic fields. The effect is self-sustaining as long as the photon momentum anisotropy is sufficiently high.

Furthermore, ponderomotive particle forcing, $\mathbf{F}_p \propto -q_e^2(m\omega)^{-1}\nabla\mathbf{E}^2$, is likely to be active in the strongly oscillatory wakefield plasma. This drift force is independent of the charge sign; both electrons and ions drift in the same manner. Such effects has been reported by other authors (Hoshino 2008; Liang & Noguchi 2007) to being responsible for the acceleration of particles due to forcing by Poynting flux pulses. The *coherent* nature of the plasma forcing by these authors, contrasts our *stochastic* forcing.

Determining how the magnetic field will decay is a challenge yet to be met; modeling a larger plasma volume is necessary to determine the ultimate temporal and spatial development. Resorting to lower-dimensional models will not solve the problem; the instability is inherently 3D in nature and cannot develop realistically in lower dimensions (cf. Frederiksen et al. 2004). We also observe in Fig. 4 that filaments, current structures and field scales are limited by the computational volume – i.e. they are 'boxed-in'. Nonetheless, they survive relatively far behind the final tail of the photon wakefield (the GRB). Both electrons and ions are responsible for the density filaments, the current densities are borne almost entirely by the electrons – again – owing to the inertial difference. We may therefore expect that as long as the photon anisotropy is "large", the field structures will survive.

We proceed to speculate that such magnetized wakefields volumes could provide 'magnetic walls' against which trailing ejecta could gradually produce a build- up of shocks and particle acceleration, as the ejecta traverses the preconditioned circumburst medium.

4. CONCLUSIONS

We emphasize the importance of bridging the gap between the (statistical) sub-Debye domain and the macroscopic Vlasov-/super-Debye domain in astrophysical plasma modeling, opening the possibility of a detailed kinetic photon description, and allowing the modeling of processes such as neutron transport and decay, neutrino streaming and transport, pair production etc. Frequencies for wave-particle collisions and for particle-particle collisions (e.g. Compton) are comparable in magnitude for the physical conditions we have considered in this Letter. In effect

$$\nu_{\mathrm{coll}} \propto \omega_{pe} = c^{-1}\delta_e \ , \ \nu_{\mathrm{bin}} \propto nc\sigma_T \ \Rightarrow \ \nu_{\mathrm{coll}} \sim \nu_{\mathrm{bin}} \ ,$$

where n is the photon number density, σ_T the Thompson cross section, l the burst light duration. Subscripts "coll" and "bin" denote "collective" (wave-particle), and "binary" (particle-particle) - respectively.

Our main findings from these first simplified GRB-CBM wakefield interaction simulations, which we have conducted with the new PHOTONPLASMA hybrid scheme described briefly in Section 2, are:

1. Strong photon density gradients plays an important role in the dynamics of the CBM while being traversed by a GRB. We therefore lend support from our studies to suggestions set

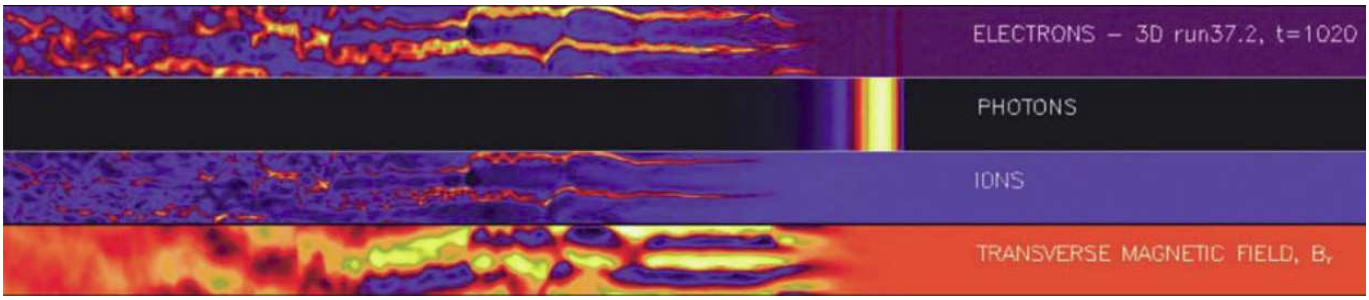

FIG. 4.— Current structures for electrons (panel 1), photon pulse (panel 2), ions (panel 3) and (transverse, out-of-plane) magnetic field structure (panel 4) in our 3D wakefield simulation, at simulation time $t = 1020\omega_{pe}^{-1} \approx 10^4\Delta t$. The GRB photon pulse has light-length $L_c \equiv c/\tau_{GRB} = 200 \approx 64\delta_e$. The computational volume has dimensions $\{L_x, L_y, L_z\} = \{40, 8, 1600\}$ or, in electron skin-depths, $\{L_x, L_y, L_z\} \approx \{12\delta_e, 2\delta_e, 500\delta_e\}$.

forth by (Barbiellini et al. 2006) to study in more detail these stochastically induced wakefield processes.

2. The GRB spectrum is locally affected by the same gradient density induced effects, and this leads to local high energy fluctuations in the GRB spectrum and light curve on sub-millisecond-to-millisecond time scales.

3. A transverse magnetic field, quasi-static in the CBM frame, is generated in the wakefield of a GRB traversing a quiescent plasma. The field scales are likely limited by our numerical capabilities to follow the growth.

It has been argued theoretically (Beloborodov 2002; Thompson & Madau 2000) that the CBM ahead of the trailing forward shock could be loaded with a relatively high density pair plasma component. From this work, and from observing Fig. 3, we see that accounting for pair production ($\gamma + \gamma \leftrightarrow e^+ + e^-$) is imperative. In future work we shall add such dynamics, to test in particular whether density fluctuations could grow and eventually lead to externally produced shocks as a consequence of γ-ray preconditioning of the circumburst medium.

Collaboration with Troels Haugbølle, Christian Hededal, and Åke Nordlund on the development of the PHOTON-PLASMA code is acknowledged. Computer time was provided by the Danish Center for Scientific Computing (DCSC).

REFERENCES

Barbiellini, G., Celotti, A., Ghirlanda, G., Longo, F., Piro, L., & Tavani, M. 2004, MNRAS, 350, L5
Barbiellini, G., Longo, F., Omodei, N., Celotti, A., & Tavani, M. 2006, in American Institute of Physics Conference Series, Vol. 836, Gamma-Ray Bursts in the Swift Era, ed. S. S. Holt, N. Gehrels, & J. A. Nousek, 91–96
Beloborodov, A. M. 2002, ApJ, 565, 808
Connaughton, V. 2002, ApJ, 567, 1028
Frederiksen, J. T. 2008, PhD thesis, Stockholm Observatory
Frederiksen, J. T., Hededal, C. B., Haugbølle, T., & Nordlund, Å. 2004, ApJ, 608, L13
Gruzinov, A. 2001, ArXiv Astrophysics e-prints, astro-ph/0111321
Haugboelle, T. 2005, ArXiv Astrophysics e-prints, astro-ph/0510292
Hededal, C. 2005, PhD thesis, Niels Bohr Institute, astro-ph/0506559
Hededal, C. B., Haugbølle, T., Frederiksen, J. T., & Nordlund, Å. 2004, ApJ, 617, L107
Hoshino, M. 2008, ApJ, 672, 940
Keshet, U., Katz, B., Spitkovsky, A., & Waxman, E. 2008, ArXiv e-prints, astro-ph/0802.3217
Kocevski, D., Ryde, F., & Liang, E. 2003, ApJ, 596, 389
Kostyukov, I., Kiselev, S., & Pukhov, A. 2003, Physics of Plasmas, 10, 4818
Liang, E., & Noguchi, K. 2007, ArXiv e-prints, astro-ph/0704.1843
Medvedev, M. V., & Loeb, A. 1999, ApJ, 526, 697
Phuoc, K. T., Burgy, F., Rousseau, J.-P., Malka, V., Rousse, A., Shah, R., Umstadter, D., Pukhov, A., & Kiselev, S. 2005, Physics of Plasmas, 12, 023101
Pines, D., & Bohm, D. 1952, Phys. Rev., 85, 338
Pukhov, A. 2000, Journal of Plasma Physics, 61, 425
Ryde, F., & Svensson, R. 2002, ApJ, 566, 210
Silva, L. O., Fonseca, R. A., Tonge, J. W., Dawson, J. M., Mori, W. B., & Medvedev, M. V. 2003, ApJ, 596, L121
Thompson, C., & Madau, P. 2000, ApJ, 538, 105
Weibel, E. S. 1959, Phys. Rev. Lett., 2, 83